ATMOSPHERIC SCIENCE LETTERS
Atmos. Sci. Let. **17**: 216–222 (2016)
Published online 25 January 2016 in Wiley Online Library
(wileyonlinelibrary.com) **DOI:** 10.1002/asl.645

RMetS
Royal Meteorological Society

A 31-year trend of the hourly precipitation over South China and the underlying mechanisms

Shenming Fu,[1] Deshuai Li,[2] Jianhua Sun,[3] Dong Si,[4] Jian Ling[5,*] and Fuyou Tian[4]

[1]*Institute of Atmospheric Physics, Chinese Academy of Sciences, International Center for Climate and Environment Sciences, Beijing, China*
[2]*College of Atmospheric Sciences, Lanzhou University, China*
[3]*Institute of Atmospheric Physics, Chinese Academy of Sciences, Laboratory of Cloud–Precipitation Physics and Severe Storms, Beijing, China*
[4]*China Meteorological Administration, National Climate Center, Beijing, China*
[5]*Institute of Atmospheric Physics, Chinese Academy of Sciences, LASG, Beijing, China*

**Correspondence to:*
J. Ling, LASG, Institute of Atmospheric Physics, Chinese Academy of Sciences, 40 Huayanli, Chaoyang District, Beijing 100029, China.
E-mail: lingjian@lasg.iap.ac.cn

Received: 6 May 2015
Revised: 7 October 2015
Accepted: 28 November 2015

Abstract

On the basis of a newly developed intensive hourly observational precipitation dataset, the precipitation trend of South China was investigated. Results indicate that the hourly precipitation over South China featured a significant increasing trend, particularly for the extreme precipitation category. The trend is mainly due to the increasing frequency of the precipitation events. A possible mechanism accounting for this increasing trend was proposed: the global warming may be the original forcing for the trend, through its modulation on activities of the western Pacific subtropical high, but the low-level vorticity is the most important direct trigger.

Keywords: hourly precipitation; vorticity budget; western Pacific subtropical high; rotated empirical orthogonal function (REOF)

1. Introduction

Heavy rainfall events are one of the most severe disastrous weathers worldwide (Tao, 1980; Karl and Knight, 1998; Zhou *et al.*, 2008; Grimm and Tedeschi, 2009; Hitchens *et al.*, 2013; Stevenson and Schumacher, 2014). Every year, the flash flood, debris flow and urban waterlogging triggered by heavy rainfall events result in substantial casualties, great economic losses and other large social consequences (Tao and Ding, 1981; Karl and Knight, 1998; Zhao *et al.*, 2004; Ramos *et al.*, 2014). Moreover, as a key component of the hydrological cycle, the precipitation is vital in determining the distribution of the water resource that participates in many physical, chemical and biogeological processes of the Earth system. Therefore, clarifying the trend of the precipitation and revealing the main mechanisms accounting for the variation of precipitation are very important in the recent climate research (Karl and Knight, 1998; Buffoni *et al.*, 1999; Black, 2009; Chen *et al.*, 2009; Yu and Li, 2012; Ramos *et al.*, 2014).

The South China, which is under the influences of the East Asian summer monsoon, the Indian Monsoon, the western Pacific subtropical high, and the dynamical/thermodynamical effects of the Tibetan Plateau, is one of the most famous and important rainy regions in Asia (Tao, 1980; Zhao *et al.*, 2004; Zhou *et al.*, 2008). In recent years, serious floods caused by torrential rainfall events occurred frequently in South China (e.g. the devastating floods in 1982, 1994, 1998, 2005 and 2008). Furthermore, many studies (Qian and Lin, 2005; Zhai *et al.*, 2005; Ren *et al.*, 2006; Fischer *et al.*, 2012) reveal that, under the background of the global climate change, the precipitation over South China show significant changes, which may render a potential increasing flood risk. Possible mechanisms accounting for the variation of precipitation were discussed, mainly focused on the El Niño Southern Oscillation (ENSO) and the Pacific Decadal Oscillation (Chan and Zhou, 2005), the tropical cyclone activities (Ren *et al.*, 2006), the variation of the East Asian summer monsoon (Ding *et al.*, 2008), the surface flux over the Indochina Peninsula and the South China Sea (Liang and Qian, 2009), the surface air temperature (Yu and Li, 2012), as well as the remote impacts of the Arctic Oscillation (Li and Leung, 2013). It should be noted that, although many factors were found to be capable of influencing/determining such variation over South China, thus far, no comparisons have been conducted among these factors. Moreover, most of the previous studies were based on sparse station observation with low temporal resolution (6-h or daily) and reanalysis data with coarse horizontal resolution ($2.5° \times 2.5°$), thus, rich features of the hourly precipitation cannot be revealed in detail. Therefore, this study intends to evaluate the trend of the hourly precipitation over South China more thoroughly using a new intensive hourly station observational rainfall dataset, and to determine the main factors accounting for the variation of hourly precipitation.

Data and methods are presented in the next section, main results are shown in Section 3, and finally a conclusion is provided in Section 4.

2. Data and methods

In this study, the hourly observational precipitation data at 2420 stations (Figure 1(a)) of the China Meteorological Administration (CMA) from 1982 to 2012 were used to determine the rainy region of South China in the warm season (from May to September) objectively, and also to calculate the trend of the hourly precipitation. Six-hourly European Centre for Medium-range Weather Forecasts Interim reanalysis (ERA-I) with a horizontal resolution of $0.75° \times 0.75°$ (Simmons *et al.*, 2007) was used for evaluating the relative importance of various factors to the rainfall event. The Rotated Empirical Orthogonal Function (REOF) analysis (Kaiser, 1958), the correlation analysis and the vorticity budget are the main research methods. The Student's *t*-test and the Mann–Kendall trend test (Mann, 1945; Kendall, 1975) were used to verify the significance of the correlation and the trend, respectively. The vorticity budget equation (Kirk, 2003) used in this study is as follows:

$$\frac{\partial \zeta}{\partial t} = \mathrm{HAV} + \mathrm{VAV} + \mathrm{TIL} + \mathrm{STR} + \mathrm{AF} \qquad (1)$$

where ζ is the vertical vorticity, HAV represents the horizontal advection of vorticity, VAV denotes the vertical advection of vorticity, TIL stands for the titling effect, STR represents the stretching effect and AF denotes the advection of the planetary vorticity (refer Appendix A for detailed information).

3. Results

3.1. The trend of hourly precipitation over South China

In this study, the REOF analysis (Horel, 1982) was conducted to detect the similar localized modes of the hourly precipitation objectively. The data scarcity of each station that was used in the REOF analysis was confined to be less than 2%. Thus, out of the 2420 stations shown in Figure 1(a), only 1095 meet the above criteria, which distribute homogenously in the middle, east and south China (not shown). As reported by Kaiser (1958), eigenvalue separations were used to test the number of region divisions, and their corresponding maximum loading vectors were used to determine the climate divisions. A total of ten spatial patterns were determined over central eastern China, with their accumulated variance contribution exceeding 60% (Li *et al.*, 2015). The rainy area over South China can be well represented by the second leading mode of the REOF analysis (Figure 1(b)) which contributes 7.84% to the total variation of precipitation over China. The blue dashed rectangle in Figure 1(b) was defined as the area of the South China, which was used to calculate the averaged value for each potential factor that may influence the precipitation over South China, based on the ERA-I reanalysis data. This region contains 99 stations; therefore, the mean hourly precipitation over South China was defined as the averaged value of the hourly precipitation of all these stations.

As reported by Karl and Knight (1998), changes in precipitation amount are determined by the change in the frequency of occurrence of precipitation events (the frequency factor) and the change in the intensity of precipitation per event (the intensity factor). In order to evaluate the precipitation trend thoroughly, the hourly precipitation intensity ($\mathrm{mm\,h^{-1}}$) was classified into ten categories. All the hourly precipitation observed in 99 stations over South China was firstly sorted from lowest to highest value and then equally divided into ten categories. That is, Category 1 represents the first 10 percentile of hourly precipitation intensity corresponding to the very light precipitation, and Category 10 stands for the last 10 percentile of hourly precipitation intensity corresponding to very intense precipitation events. The trends of these ten categories were calculated following Karl and Knight (1998), and an increasing trend was detected for all categories. The hourly precipitation in categories from five to ten accounts for up to 96.9% of the total precipitation amount during the warm season (Table 1). Therefore, the variation of the precipitation over South China was dominated by these categories, and their trends are discussed in detail (Figure 2(a)).

As Figure 2(a) illustrates, all the categories from five to ten featured an increasing trend, which is dominated by the frequency factor. This means that the increasing trend of the hourly precipitation over South China was mainly because of the growth in the number of the precipitation events, whereas the intensity of the precipitation event changed slightly, except for the extreme precipitation category. The time series of the extreme precipitation events over South China during the last 31 years are shown in Figure 2(b). It clearly shows the remarkable increasing trend exceeding the 95% confidence level. It is obvious that, the category with larger intensity of the precipitation has larger increasing trend. For the extreme precipitation category (the Category 10), which accounted for about 57.1% of the total precipitation amount and generally featured a mean precipitation rate of $14.73\,\mathrm{mm\,h^{-1}}$ (Table 1), has the largest increasing trend as well as its corresponding frequency and intensity factors. Moreover, the intensity factor account for about 10% of the total increasing trend (Figure 2(a)). It suggests that the extreme hourly precipitation events over South China featured a significant growth in their total number and a weak increasing in their intensity, both of which may increase the flood risk over South China remarkably.

3.2. The dominant factors for the hourly precipitation over South China

In order to determine the dominant factors accounting for the variation of precipitation, the factors proven to be capable of influencing/dominating the rainfall events over South China through detailed case studies (Tao, 1980; Zhao *et al.*, 2004; Xia *et al.*, 2006; Xia and

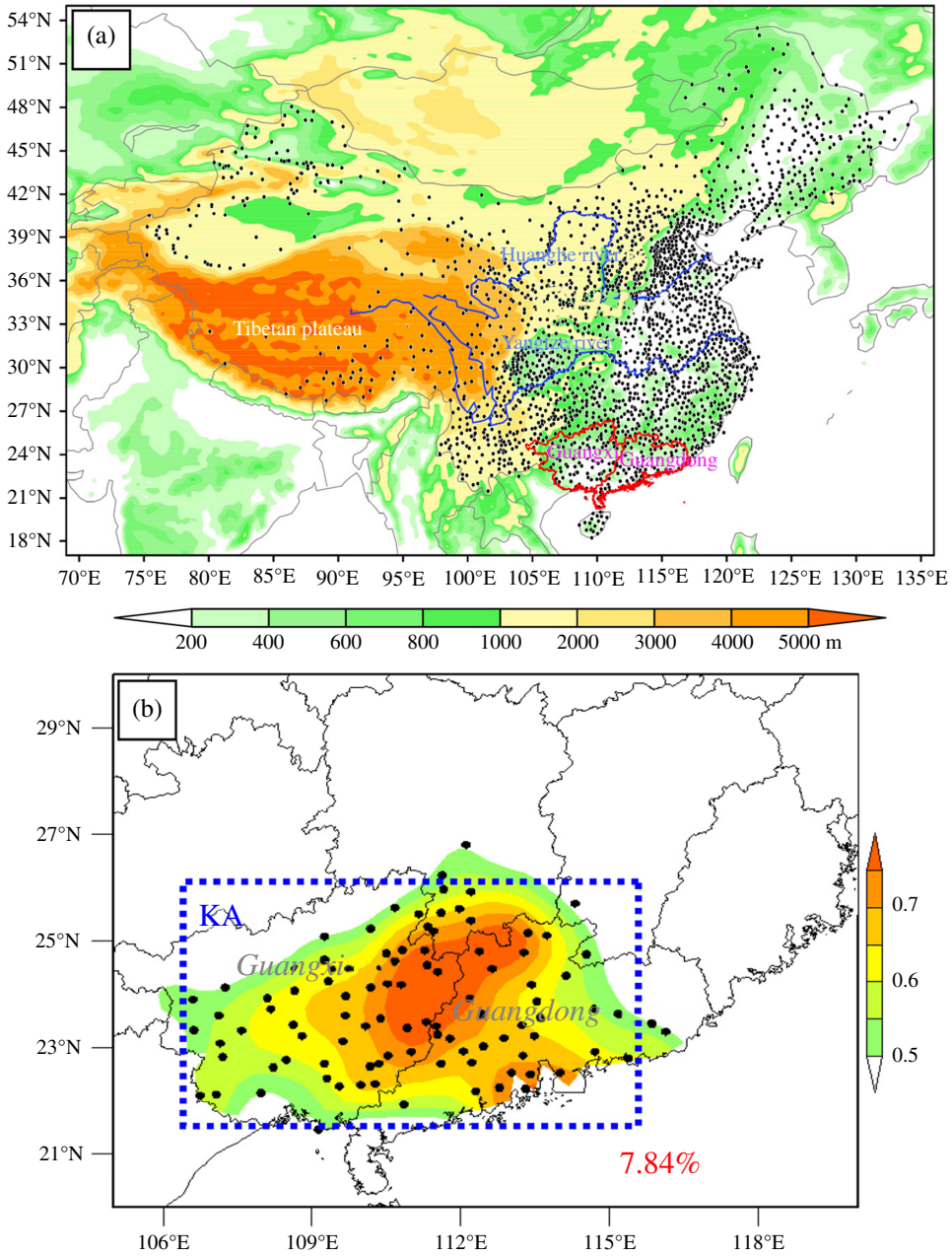

Figure 1. (a) Stations with hourly precipitation observation (black dots) and the terrain characteristics (shaded, units: m). (b) The forth leading mode derived from hourly precipitation during the period of 1982–2012 (the shaded illustrates the value of the loading vector). The blue rectangle represents the area of South China used in this study.

Table 1. The contribution rate (CR, %) of each category to the total precipitation amount in the warm season, and the averaged intensity (AI, mm h^{-1}) of each category.

Category	5	6	7	8	9	10	5–10
CR (%)	2.1	3.5	5.8	9.9	18.5	57.1	96.9
AI (mm h^{-1})	0.6	0.95	1.54	2.59	4.83	14.73	4.21

Zhao, 2009; Zhao and Wang, 2009; Fu *et al.*, 2010) had been evaluated using the 6-h ERA-I reanalysis data. Because the time interval of the ERA-I analysis was 6 h, the hourly precipitation at 0000, 0600, 1200 and 1800 UTC was used to calculate the correlation with each possible factor.

In this study, 20 factors suggested by previous studies were evaluated, including vertical velocity (VV), vorticity (VOR), vertical helicity (HEL), front/baroclinity (BAR) denoted by $|\nabla_h T|$, where ∇_h is the horizontal gradient operator and TEM is the temperature, divergence of the moisture transport (DMT), temperature (TEM), temperature advection (TA), baroclinic conversion term between the available potential energy and kinetic energy (Lorenz, 1955), convective instability, convective available potential energy, thickness between 925 and 500 hPa, specific humidity, entire atmosphere precipitable water, potential vorticity, surface pressure, zonal wind, meridional wind, horizontal wind velocity, surface latent heat flux and surface sensible heat flux. It should be noted that, all

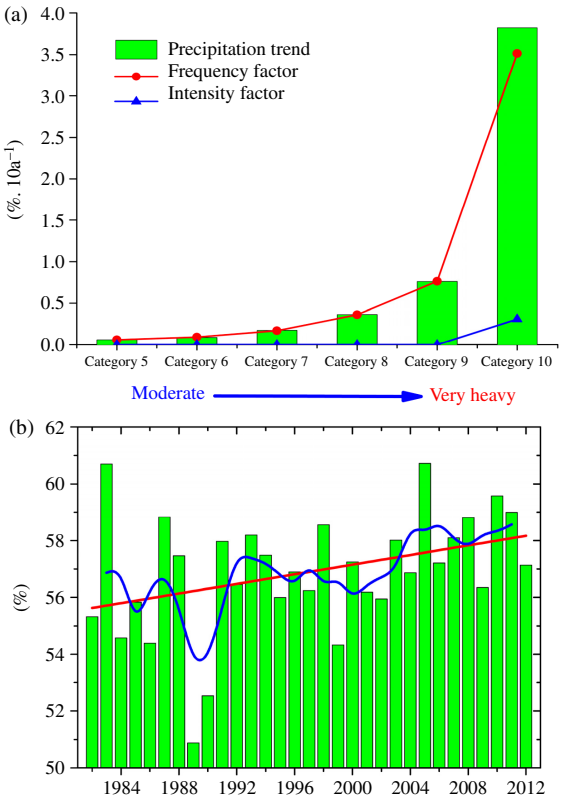

Figure 2. (a) Precipitation trend of each category (10^{-1}% year^{-1}), with their corresponding contribution from frequency and intensity factor respectively. (b) Time series of the contribution (%) of the hourly precipitation in Category 10 to the total precipitation over South China, where the blue curve is the smoothed curve (using a 9-point binomial filter), and the red line is its linear trend.

the three-dimensional variables were calculated at ten successive vertical levels from 925 to 500 hPa, and the convective instability were calculated between 925 and 500 hPa, 900 and 700 hPa, 700 and 500 hPa, 900 and 800 hPa, as well as 800 and 700 hPa, respectively.

The maximum correlation coefficient of each factor was identified (for the three-dimensional variable, the correlation coefficients is different for different level), and then sorted from large to small. In this study, only eight factors can be regarded as in good correlation with the hourly precipitation passing the significant test at 95% level. They are the seven factors shown in Figure 3, and the convective instability calculated between 900 and 700 hPa with a correlation coefficient of −0.215. All other factors featured correlation coefficients below 0.11, and thus were not discussed in this study. Among all the eight factors, VOR has the maximum correlation coefficient among the levels between 925 and 600 hPa (Figure. 3), whereas VV has the largest correlation at 550 hPa, slightly greater than that of VOR. Thus, overall, VOR was the most important factor that impacts the hourly precipitation over South China. As Figure 3 illustrates, DMT at 900 hPa ranks the third place (−0.245). DMT was in negative correlation with the precipitation below 750 hPa, implying the importance of low-level moisture convergence to the precipitation; whereas positive correlation appeared above 750 hPa, indicating the importance of divergence at higher levels to the precipitation. In addition, the non-divergent level was mainly located around 750 hPa. The convective instability, HEL, TA, TEM and BAR rank from the forth to eighth place respectively. It reveals that convective unstable layer, positive helicity, warm TA, cold low-level temperature and strong baroclinity are generally conducive to the precipitation over South China.

The maximum correlation (0.442) between VOR and precipitation is at 850 hPa, therefore, the low-level vorticity, that is closely related to the shear lines (Zhao *et al.*, 2004), the quasi-stationary front (Tao, 1980; Xia and Zhao, 2009), the mesoscale vortices (Tao, 1980; Fu *et al.*, 2010) and the tropical disturbance/cyclones (Zhao *et al.*, 2004) is vital in triggering the precipitation over South China. Because the variation of VOR is governed by the vorticity budget equation, the correlation coefficients between each vorticity budget term on the right hand side of the Equation (1) and VOR were evaluated. It indicates that STR was highly correlated with VOR, with a correlation coefficient up to 0.636, which means that the convergence was the dominant factor for the maintenance of positive vorticity at lower level. HAV ranks the second place (−0.259), implying HAV is the most detrimental factor consuming the positive vorticity. It should be noted that, the above results were also confirmed by many case studies (Zhao *et al.*, 2004; Fu *et al.*, 2010).

3.3. Mechanisms of the trend of hourly precipitation

In order to explore the hourly precipitation trend over South China, correlation between the 850-hPa VOR and hourly precipitation as well as the variance of the 850-hPa VOR were calculated during the warm season of each year (613 samples per year). As Figure 4(a) illustrates, every year, VOR was generally well correlated with the hourly precipitation, particularly for the year 1982 (0.511), 1994 (0.529), 1998 (0.521), 2002 (0.539), 2006 (0.515), 2008 (0.516) and 2009 (0.548), whereas 1991 features the smallest correlation coefficient (0.231), when a severe drought appeared over South China. The annual correlation coefficient between VOR and the hourly precipitation features an increasing trend (exceeds the 90% confidence level), which means that the low-level vorticity may become more important in the rainfall events over South China. The annual variance of VOR generally featured an increasing trend (Figure 4(b)), exceeding the 95% confidence level. This implies that, the weather systems directly triggered the rainfall events (e.g. the synoptical, subsynoptical, mesoscale weather systems, etc.) generally became more frequent and/or stronger. Therefore, the vorticity related perturbation circulations generally became more favorable for the rainfall events over South China. It might be the reason for the increasing trend of hourly precipitation there. Moreover, from Figure 4(a) and (b), it is obvious that, overall, the

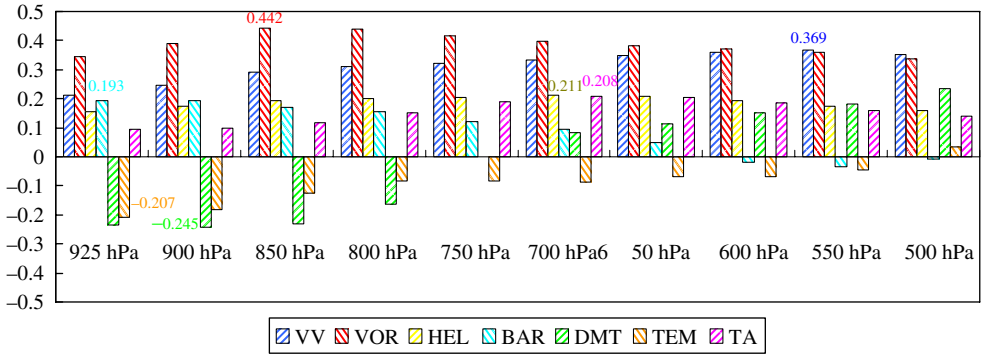

Figure 3. Correlation between the mean hourly precipitation and the seven factors averaged over South China at different levels. The maximum correlation coefficient of each factor is marked with corresponding color.

stronger the annual variance of VOR, the larger the correlation coefficient (their correlation coefficient is 0.48), which also confirms that, the vorticity related perturbation circulations were very important in triggering the rainfall events over South China.

From Figure 4(c), the longitude of westernmost ridge point of the western Pacific subtropical high features a decreasing trend (exceeds the 90% confidence level), implying that the subtropical high generally stretched more westward and thus influenced wider areas over South China. Therefore, the circulations associated with the subtropical high became more favorable for the divergence around 500 hPa over South China, which can be confirmed by the significant increasing trend (exceeding the 90% confidence level) of averaged divergence at 500 hPa over South China (Figure 4(d)). Because the non-divergent level was mainly located around 750 hPa (Figure 3), according to the continuity equation, the stronger divergence around 500 hPa favors stronger convergence at lower levels. This result can be confirmed by the correlation coefficient between the divergence at 500 and 850 hPa for 31 years with a value of −0.38 (above the 95% confidence level). Because STR dominated the variation of vorticity (Section 3.2), stronger lower-level convergence were more conducive to the occurrence/enhancement of positive vorticity related anomalous circulation, therefore, the low-level VOR's variance shows an increasing trend (Figure 4(b)), which may account for the increasing trend of the precipitation over South China (Figure 3).

4. Conclusion and discussion

In this study, on the basis of a new intensive hourly observational precipitation dataset during the warm seasons of 1982–2012, the rainy region over South China was determined objectively using REOF analysis. The trend of the hourly precipitation over South China was investigated in detail by calculating both frequency and intensity factors. A significant increasing trend was detected in the hourly precipitation over South China, particularly for the extreme precipitation category, which accounts for about 57.1% of the total precipitation. Generally, the increasing trend was due to the growth in the number of the precipitation events; whereas for the extreme precipitation events, an increase of about 10% in the precipitation intensity was also significant, which may increase the risk of flooding over South China remarkably.

A total of 20 factors proven to determine/influence the precipitation by previous case studies were evaluated. The results reveal that the non-divergent level was mainly located around 750 hPa over South China and the low-level vorticity was the key factor influencing the hourly precipitation. The low-level shear lines, quasi-stationary front, mesoscale vortices and tropical disturbance/cyclones are vital in triggering the precipitation over South China directly. The vorticity budget was used to understand the variation of VOR, and STR which is determined by the divergence was found to be the dominant factor.

A possible mechanism accounting for the increasing trend of the hourly precipitation over South China is proposed. The western Pacific subtropical high stretched more westward during the last 31 years, which favored the divergence at higher levels over South China. Thus, low-level convergence was enhanced, which rendered an increasing trend of VOR in the lower level through term STR. This increasing trend in the low-level vorticity was corresponding to the increasing and/or intensifying of the weather systems that triggered the precipitation directly. Thus the precipitation over South China shows an increasing trend.

Recently, He and Zhou (2015) proposed that, the change in the zonal sea surface temperature gradient between the tropical Indian Ocean and the tropical western Pacific which is closely related to the global warming, dominated the variation of the intensity of the western Pacific subtropic high. Therefore, the global warming may be the original forcing for the increasing trend of hourly precipitation over South China through its modulation on activities of the western Pacific subtropical high.

Acknowledgements

The authors thank the European Centre for Medium-range Weather Forecasts and China Meteorological Administration

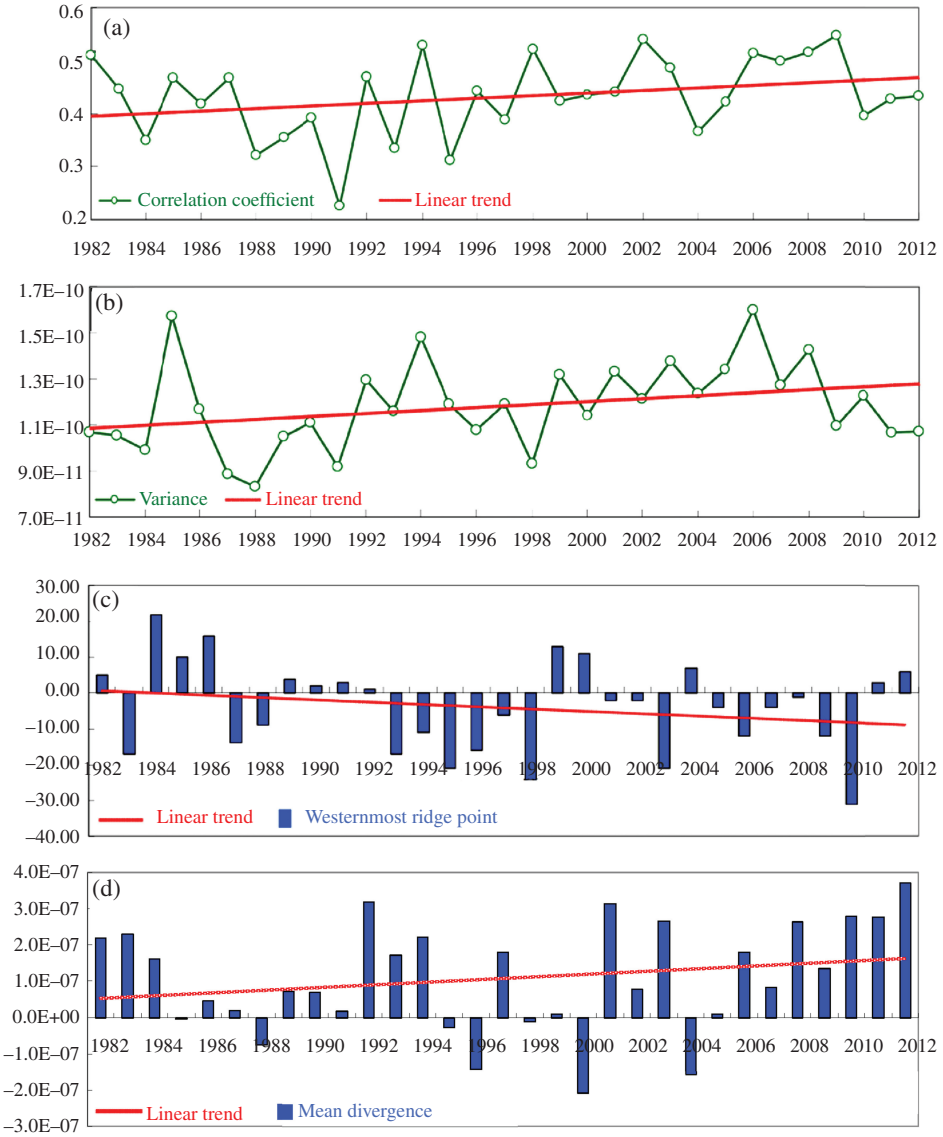

Figure 4. (a) Annual correlation between the averaged VOR at 850 hPa and the mean hourly precipitation over South China; (b) the annual variance of the vorticity at 850 hPa over South China (units: s^{-2}); (c) the anomaly of the westernmost ridge point of the western Pacific subtropical high; and (d) the annual mean divergence at 500 hPa (units: s^{-1}) over South China.

for providing the data. The authors also thank Editor Yan Yin and two anonymous reviewers for their valuable suggestions. This research was supported by the National Key Basic Research and Development Project of China (2012CB417201 and 2015CB453200) and the National Natural Science Foundation of China (41205027, 41375053 and 41575062).

Appendix A: The vorticity budget equation

The vorticity budget equation is following Kirk (2003):

$$\frac{\partial \zeta}{\partial t} = -\mathrm{V}_h \cdot \nabla_h \zeta - \omega \frac{\partial \zeta}{\partial p} + \mathbf{k} \cdot \left(\frac{\partial \mathrm{V}_h}{\partial p} \times \nabla_h \omega \right) - (\zeta + f) \nabla_h \cdot \mathrm{V}_h - \beta v$$

HAV VAV TIL STR AF

where ζ is the vertical vorticity; $\mathbf{V}_h = u\mathbf{i} + v\mathbf{j}$ is the horizontal velocity vector, **i, j, k** stand for the unit vector points to the east, north and zenith respectively; $\nabla_h = \frac{\partial}{\partial x}\mathbf{i} + \frac{\partial}{\partial y}\mathbf{j}$ is the horizontal gradient operator; f is the Coriolis parameter; p is the pressure; $\omega = dp/dt$ and $\beta = \partial f/\partial y$.

References

Black E. 2009. The impact of climate change on daily precipitation statistics in Jordan and Israel. *Atmospheric Science Letters* **10**: 192–200, doi: 10.1002/asl.233.

Buffoni L, Maugeri M, Nanni T. 1999. Precipitation in Italy from 1833 to 1996. *Theoretical and Applied Climatology* **63**: 33–40.

Chan JCL, Zhou W. 2005. PDO, ENSO and the early summer monsoon rainfall over south China. *Geophysical Research Letters* **32**: L08810, doi: 10.1029/2004GL022015.

Chen H, Zhou T, Yu R, Li J. 2009. Summer rain fall duration and its diurnal cycle over the US Great Plains. *International Journal of Climatology* **29**: 1515–1519.

Ding Y, Wang Z, Sun Y. 2008. Inter-decadal variation of the summer precipitation in East China and its association with decreasing Asian summer monsoon. Part I: observed evidences. *International Journal of Climatology* **28**: 1139–1161.

Fischer T, Gemmer M, Liu L, Su B. 2012. Change-points in climate extremes in the Zhujiang River Basin, South China, 1961–2007. *Climatic Change* **110**: 783–799, doi: 10.1007/s10584-011-0123-8.

Fu SM, Zhao SX, Sun JH, Li WL. 2010. One kind of vortex causing heavy rainfall during pre-rainy season in South China. *Chinese Journal of Atmospheric Sciences* **34**: 235–252, doi: 10.3878/j.issn.1006-9895.2010.02.01.

Grimm AM, Tedeschi RG. 2009. ENSO and extreme rainfall events in South America. *Journal of Climate* **22**: 1589–1609.

He C, Zhou TJ. 2015. Responses of the western North Pacific Subtropical High to global warming under RCP4.5 and RCP8.5 scenarios projected by 33 CMIP5 models: the dominance of tropical Indian Ocean – tropical western Pacific SST gradient. *Journal of Climate* **28**: 365–380, doi: 10.1175/JCLI-D-13-00494.1.

Hitchens NM, Brooks HE, Schumacher RS. 2013. Spatial and temporal characteristics of heavy hourly rainfall in the United States. *Monthly Weather Review* **141**: 4564–4575, doi: 10.1175/MWR-D-12-00297.1.

Horel JD. 1982. A rotated principal component analysis of the interannual variability of the Northern Hemisphere 500 mb height field. *Monthly Weather Review* **109**: 2080–2092.

Kaiser HF. 1958. The varimax criterion for analytic rotation in factor analysis. *Psychometrika* **23**: 187–200.

Karl TR, Knight RW. 1998. Secular trends of precipitation amount, frequency, and intensity in the United States. *Bulletin of the American Meteorological Society* **79**: 231–241.

Kendall MG. 1975. *Rank Correlation Methods*. Charles Grifin Company: London.

Kirk JR. 2003. Comparing the dynamical development of two mesoscale convective vortices. *Monthly Weather Review* **131**: 862–890.

Li YF, Leung LR. 2013. Potential impacts of the Arctic on interannual and interdecadal summer precipitation over China. *Journal of Climate* **26**: 899–917, doi: 10.1175/JCLI-D-12-00075.1.

Li DS, Sun JH, Fu SM, Wei J, Wang SG, Tian FY. 2015. Spatiotemporal characteristics of hourly precipitation over central eastern China during the warm season of 1982–2012. *International Journal of Climatology*, doi: 10.1002/joc.4543.

Liang N, Qian YF. 2009. Interdecadal change in extreme precipitation over South China and its mechanism. *Advances in Atmospheric Sciences* **26**: 109–118.

Lorenz EN. 1955. Available potential energy and the maintenance of the general circulation. *Tellus* **7**: 157–167.

Mann HB. 1945. Nonparametric tests against trend. *Econometrica* **13**: 245–259, doi: 10.2307/1907187.

Qian W, Lin X. 2005. Regional trends in recent precipitation indices in China. *Meteorology and Atmospheric Physics* **90**: 193–207.

Ramos AM, Trigo RM, Liberato MLR. 2014. A ranking of high-resolution daily precipitation extreme events for the Iberian Peninsula. *Atmospheric Science Letters* **15**: 328–334, doi: 10.1002/asl2.507.

Ren F, Wu G, Dong W, Wang X, Wang Y, Ai W, Li W. 2006. Changes in tropical cyclone precipitation over China. *Geophysical Research Letters* **33**: L20702, doi: 10.1029/2006GL027951.

Simmons A, Uppala S, Dee D, Kobayashi S. 2007. ERA-Interim: new ECMWF reanalysis products from 1989 on-wards. ECMWF Newsletter No. 110, ECMWF, Reading, UK, 25–35.

Stevenson SN, Schumacher RS. 2014. A 10-year survey of extreme rainfall events in the Central and Eastern United States using gridded multisensor precipitation analyses. *Monthly Weather Review* **142**: 3147–3162.

Tao SY. 1980. *Rainstorms in China*. Science Press: Beijing.

Tao SY, Ding YH. 1981. Observational evidence of the influence of the Qinghai–Xizang (Tibet) Plateau on the occurrence of heavy rain and severe convective storms in China. *Bulletin of the American Meteorological Society* **62**: 23–30.

Xia RD, Zhao SX. 2009. Diagnosis and modeling of meso-β-scale systems of heavy rainfall in warm sector ahead of front in South China (Middle part of Guangdong Province) in June 2005. *Chinese Journal of Atmospheric Sciences* **33**: 468–488, doi: 10.3878/j.issn.1006-9895.2009.03.06.

Xia RD, Zhao SX, Sun JH. 2006. A study of circumstances of meso-β-scale systems of strong heavy rainfall in warm sector ahead of fronts in South China. *Chinese Journal of Atmospheric Sciences* **30**: 988–1008, doi: 10.3878/j.issn.1006-9895.2006.05.26.

Yu RC, Li J. 2012. Hourly rainfall changes in response to surface air temperature over eastern contiguous China. *Journal of Climate* **25**: 6851–6861, doi: 10.1175/JCLI-D-11-00656.1.

Zhai PM, Zhang X, Wan H, Pan X. 2005. Trends in total precipitation and frequency of daily precipitation extremes over China. *Journal of Climate* **18**: 1096–1108.

Zhao YC, Wang YH. 2009. A review of studies on torrential rain during pre-summer flood season in South China since the 1980's. *Torrential Rain and Disasters* **28**: 193–202.

Zhao SX, Tao ZY, Sun JH, Bei NF. 2004. *Study on Mechanism of Formation and Development of Heavy Rainfalls on Meiyu Front in Yangtze River*. China Meteorological Press: Beijing.

Zhou TJ, Yu RC, Chen HM, Dai AG, Pan Y. 2008. Summer precipitation frequency, intensity, and diurnal cycle over China: a comparison of satellite data with rain gauge observations. *Journal of Climate* **21**: 3997–4010.